A Quantitative ^{1}H NMR Method for the Determination of Alkoxyamine Dissociation Rate Constants in Stable Free Radical Polymerization. Application to Styrene Dimer Alkoxyamines

Lichun Li, Gordon K. Hamer, and Michael K. Georges*

Department of Chemical and Physical Sciences, University of Toronto at Mississauga, 3359 Mississauga Road, Mississauga, Ontario, Canada L5L 1C6

Received July 26, 2006; Revised Manuscript Received October 3, 2006

ABSTRACT: A high-resolution ^{1}H NMR method was developed and applied to the determination of the dissociation rate constants (k_d values) of seven stable free radical polymerization (SFRP) model compounds, including three pairs of styrene dimer alkoxyamines, using oxygen as the alkyl radical scavenger. The efficiency and completeness of oxygen irreversible trapping were tested by taking advantage of the diastereoisomerism of the dimer alkoxyamines. The effects of alkoxyamine stereochemistry on the C−ON bond dissociation kinetics were also demonstrated. The ^{1}H NMR method was validated by comparing k_d values obtained by this method with ESR and HPLC results previously reported for 2,2,6,6-tetramethyl-1-(1-phenylethoxy)piperidine, a commonly studied alkoxyamine. In contrast to ESR methods, the ^{1}H NMR procedure allows for the simultaneous determination of multiple k_d values in a single experiment.

Introduction

Over the past two decades, three major living radical polymerization (LRP) processes[1] have been developed for the synthesis of structurally well-defined polymers with predetermined molecular weights and narrow polydispersities: stable free radical polymerization (SFRP), also known as nitroxide-mediated polymerization (NMP);[2−5] atom transfer radical polymerization (ATRP);[6,7] and reversible addition fragmentation chain transfer (RAFT) polymerization.[8−10] Of particular interest to us is the "classical" SFRP process, i.e., polymerization carried out in the presence of an initiating species, monomer, and a stable free radical trap.[3]

The main kinetic scheme of the SFRP process involves monomer (M), a dynamic equilibrium between a dormant polymeric alkoxyamine (P_n−T) and a transient propagating alkyl radical ($P_n^\bullet$), and a persistent (nitroxide) radical ($T^\bullet$), as shown in Scheme 1.

The rate constants, k_d and k_c, for the dissociation/activation of the dormant chains into radicals and for the reverse deactivation/coupling reaction, respectively, influence the degree of livingness of the polymerization, the molecular weight control of the resulting polymer, and the monomer conversion rate. To obtain living, well-controlled polymerization reactions, these rate constants must favorably interrelate with the propagation rate constant (k_p), the termination rate constant (k_t), the initial initiator/alkoxyamine concentration and the rate of any additional radical generation reactions. In principle, knowledge of these rate constants and the factors controlling them enables a preassessment of the potential success of a given SFRP process. Comprehensive kinetic analyses of the SFRP/NMP process have been carried out by both Fischer et al.[11,12] and Goto and Fukuda.[13]

Methods for measuring k_d can be classified into five main groups according to the instrumentation employed: HPLC,[14,15] ESR,[16−18] GPC/SEC,[19−21] alkoxyamine fluorescence quenching,[22] and ^{31}P NMR.[23] Any measurement of the true alkoxyamine decay rate requires a prompt, complete, and irreversible scavenging of the transient radical to avoid prolongation of the alkoxyamine lifetime due to the persistent radical effect.[24] In the absence of an efficient radical scavenger the experimentally determined value of k_d will be underestimated. In the HPLC method utilized by Scaiano et al.[14] and by Moad and Rizzardo[15] transient alkyl radicals were trapped with an excess of a nitroxide structurally different from the nitroxide moiety of the original alkoxyamine. Quantitative ESR spectroscopic k_d values were determined by monitoring the liberation of nitroxide radical in the presence of carbon-centered radical scavengers such as oxygen or galvinoxyl.[16−18] In the GPC method, transient radicals were scavenged by propagation in the presence of monomer; k_d values were obtained directly by GPC curve-resolution methods[19] or, indirectly, by a polydispersity evolution method.[21]

Scheme 1. Kinetic Scheme for the SFRP Process

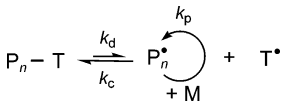

Bertin et al.[23] have reported the use of ^{31}P NMR spectroscopy to determine k_d for β-phosphorylated alkoxyamines in the presence of various alkyl radical scavengers or nitroxide reductants. The NMR method is particularly attractive because it allows the measurement of k_d by monitoring the alkoxyamine disappearance rate without consideration of the thermal stability of the liberated nitroxide**.** However, at present this approach has been limited to phosphorus-containing alkoxyamines. To overcome this limitation and extend the advantages of the NMR technique to a broader range of alkoxyamines, we have investigated the use of ^{1}H NMR to examine C−ON bond dissociation rates. Values of k_d were determined by monitoring the rate of alkoxyamine disappearance upon heating in the presence of molecular oxygen as the transient radical scavenger.

As part of a larger study of the chain-length and nitroxide structure dependence of SFRP activation/deactivation and termination processes, three pairs of styrene dimer alkoxyamines were synthesized and employed as models to mimic the polymer

* Corresponding author: Ph 905-828-5228; Fax 905-828-5425; e-mail mgeorges@utm.utoronto.ca.

10.1021/ma061700c CCC: $33.50
Published on Web 11/20/2006

Chart 1. SFRP Model Compounds

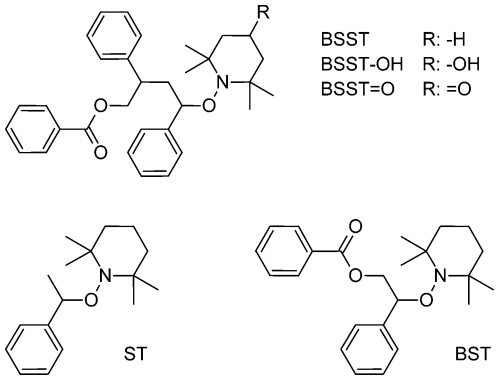

chain behavior of the C−ON bond dissociation kinetics. These models (shown in Chart 1) consist of a benzoyloxy (B) initiating end, two styryl (S) units, and a TEMPO, 4-oxo-TEMPO, or 4-hydroxy-TEMPO nitroxide cap. The models are thus identified as BSST, BSST═O, and BSST−OH, respectively. To validate the accuracy of our ^{1}H NMR method, we also determined the kinetic parameters of a common benchmark alkoxyamine model, PhEt-TEMPO (herein referred to as ST),[25] and compared our results with those previously reported using HPLC[14] and ESR spectroscopy.[16]

The rationale for the utilization of the BSS alkoxyamines was twofold. In comparison with ST the additional styryl unit introduced in the dimer model provides a more realistic environment for the chain-end benzylic radical involved in the reversible C−ON bond homolysis. This model is expected to better emulate the real polymer chain kinetic behavior in the C−ON bond dissociation reaction. Scaiano et al. have proposed 1,3-diphenyl-1-propane ("penultimate" model initiator) as a chain end mimic; however, as the authors noted, the ideal model would require an additional substituent at C-3.[26] Our dimer models meet this ideal requirement. Moreover, the styrene dimer alkoxyamines are intermediates in the SFRP process using benzoyl peroxide (BPO), or the unimer BST, as the initiator. Another notable feature of this model is that because each molecule contains two stereogenic centers, each dimer exists as a pair of diastereoisomers. Separation of the diastereoisomers by column chromatography provided materials that enabled a unique opportunity to study the effect of propagating radical stereochemistry on the C−ON bond dissociation kinetics. In addition, the fast equilibrium between the diastereoisomers was exploited in the C−ON bond dissociation kinetic studies as a probe of oxygen trapping efficiency of the alkyl radicals formed in the reaction. The oxygen trapping efficiency and its completeness could be detected with any of the pure diastereoisomers in situ by monitoring the appearance of the counterpart diastereoisomer during the C−ON bond dissociation reaction. The appearance of the counterpart diastereoisomer would indicate inefficient alkyl radical trapping.

There are two additional distinguishing features associated with the ^{1}H NMR methodology: First, provided the examination temperature is properly chosen, this method is applicable to all alkoxyamines containing ^{1}H nuclei with high spectrum resolution and sensitivity (signal/noise ratio). Second, because of the efficiency of oxygen quenching, the method allows for the possibility of independently monitoring the C−ON bond dissociation rates of several species (e.g., two diastereoisomers) at the same time in one experiment.

Experimental Section

Materials. All reagents and solvents used in the synthesis of the styrene dimer models were purchased from Aldrich and used without further purification. ST, 2,2,6,6-tetramethyl-1-(1-phenylethoxy)piperidine, was purchased from Binrad Industries Inc. and recrystallized from ethanol before use. Hexamethyldisiloxane (HMDS) and *p*-xylene-d_{10} (99+ at. % D) were also purchased from Aldrich and used as received. Oxygen (U.S.P. ≥99%) was provided by BOC Canada.

Synthesis. BST [2-phenyl-2-(2,2,6,6-tetramethylpiperidin-1-yloxy)ethyl benzoate] was synthesized from BPO, styrene, and TEMPO by a low-temperature procedure previously developed in our laboratory (to be published elsewhere). BSST was synthesized by reacting BST with 5 equiv of styrene in chlorobenzene for 6 h at 120 °C. The two BSST diastereoisomers were separated from the reaction mixture and from each other by silica gel column chromatography. One isomer (arbitrarily labeled d1) crystallized; the other (d2) remained an oil. The purity of each diastereoisomer, as measured by ^{1}H NMR, was ≥98%. BSST═O and BSST−OH were synthesized in chlorobenzene solution by an exchange reaction between BSST and 5 equiv of 4-oxo-TEMPO or 4-hydroxy-TEMPO, respectively. The two BSST═O isomers were also successfully separated by column chromatography, but under a variety of conditions, the BSST−OH diastereomers could not be resolved. As with BSST, one BSST═O isomer crystallized (d1) and the other (d2) remained an oil. All the alkoxyamine dimer models were fully characterized by 500 MHz ^{1}H NMR and 125 MHz ^{13}C NMR (Varian Unity INOVA-500 spectrometer) using a combination of 1- and 2-D (gCOSY, NOESY/EXSY, gHSQC and gHMBC) techniques;[27] ^{1}H NMR characterization spectra of the BSST, BSST═O, and BSST−OH diastereomers are available as Supporting Information. BSST-d1 and BSST═O-d1 were also characterized by single-crystal X-ray diffraction. More complete details of the alkoxyamine syntheses and characterization will be included in a future publication.

NMR Sample Preparation. *(1) Diastereoisomer Interconversion Experiments.* Diastereoisomer interconversion samples were prepared by dissolving 1.4×10^{-3} mmol of the alkoxyamine in 0.7 mL of *p*-xylene-d_{10} in a 5 mm J. Young valve-equipped NMR tube (535-JY-7, Wilmad LabGlass). The solutions were degassed by four liquid nitrogen freeze−pump−thaw cycles, and the valve was closed under vacuum. The sample tubes were immersed for a prescribed time interval in a preheated VWR 1130-1S constant temperature oil bath maintained at 100 °C (temperature stability ±0.05 °C), quenched in ice−water and then analyzed at an NMR probe temperature of 20 °C. The heat−quench−measure cycle was repeated until thermodynamic equilibrium was reached.

(2) k_d Measurements. Samples were prepared as described above except that the sample concentration was 10 mM and HMDS (∼1 mmol) was added as an internal integration standard. After degassing, each sample was saturated with oxygen gas by bubbling O_2 through the solution for 40 min, after which the NMR tubes were sealed under 1 atm of O_2. Measurements were made at five temperatures (80, 90, 100, 110, 120 °C) using the heat−quench−measure procedure. Typically, spectra were recorded until 80−90% of the original alkoxyamine was consumed.

Quantitative Data Acquisition. Quantitative ^{1}H spectra were measured on a Varian INOVA-500 spectrometer at a controlled temperature of 20 ± 0.1 °C. Spectra were acquired with a spectral width of 10 ppm, 4.9 μs (π/4) pulse width, 3 s acquisition time, 4 s delay time, and digital filtering. Depending on the S/N of the spectra, 16−64 scans were recorded. Spin−lattice relaxation times were measured[27] before and after each kinetic experiment. Typical relaxation times for the peaks of interest for each dimer were 0.5−1 s. The acquisition time of 3 s together with the π/4 pulse width and 4 s delay ensured full FID relaxation without truncation.

NMR Data Processing. All postacquisition data processing was performed with the MestReC NMR software package.[28] The raw fid was zero-filled to 64K data points, Fourier transformed, manually phased, and baseline corrected using a third-order Bernstein polynomial function. Peak intensities (integrated areas) were measured using the MestReC iterative line-fitting procedure in order to minimize subjective influences on the manual integration of peaks of interest.[28]

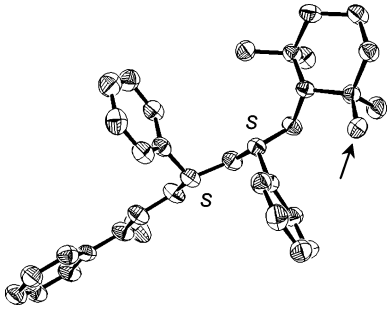

Figure 1. Single-crystal X-ray diffraction structure of the BSST-d1 (*S*,*S*) enantiomer. The arrow indicates the methyl group whose ^{1}H resonance was monitored in the kinetic experiments.

Scheme 2. BSST Diastereoisomer Interconversion

$$\text{d1} \underset{k_{c1}}{\overset{k_{d1}}{\rightleftharpoons}} \text{BSS}^{\bullet} + \text{T}^{\bullet} \underset{k_{d2}}{\overset{k_{c2}}{\rightleftharpoons}} \text{d2}$$

Kinetic Data Analysis. The reaction kinetics were followed using the ratio of the lowest frequency methyl peak (ca. 0.5 ppm) on the TEMPO moiety of the alkoxyamines[29] to the internal standard HMDS. First-order exponential line fitting was performed with Origin 7.0 for the dimeric alkoxyamine interconversion kinetics. For the alkoxyamine C−ON bond dissociation kinetics, k_d values were obtained from the slope of the least-squares linear regression line of $\ln(I/I_0)$ vs time, where I_0 is the initial alkoxyamine concentration and I is the concentration measured after any prescribed reaction time.

Results and Discussion

Absolute Configuration of the Styrene Dimer Alkoxyamines. The two pairs of diastereoisomers belonging to BSST and BSST═O were separated successfully with column chromatography. The crystalline diastereomers were arbitrarily labeled as d1 isomers (BSST-d1 and BSST═O-d1) and the oily viscous diastereomers as d2 (BSST-d2 and BSST═O-d2). The absolute stereoconfigurations of the two d1 isomers were determined to be a racemic mixture of (*R*,*R*) and (*S*,*S*) enantiomers by X-ray crystallography. The d2 isomers are therefore a mixture of (*R*,*S*) and (*S*,*R*) enantiomers. The single-crystal structure of the BSST-d1 (*S*,*S*) enantiomer is shown in Figure 1. It is of interest to note that even though the configuration of the two stereocenters are both *S*, the two phenyl groups are located on the opposite side of the zigzag backbone chain of the molecule. The solution conformation of BSST-d1 is similar to that of the X-ray structure, based on an analysis of backbone vicinal ^{1}H−^{1}H coupling constants. Another notable feature of the dimer models is that, due to the aromatic ring-current shielding effect of the phenyl ring of the terminal styrene monomer unit, one of the four methyl peaks (indicated by the arrow in Figure 1) is well separated from the other three in the ^{1}H NMR spectrum. Generally, this lowest frequency methyl peak was employed for quantitative kinetic data analysis, although any reasonably well-resolved peak(s) of the alkoxyamine could be used.

Diastereoisomeric Interconversion Kinetics of the Styrene Dimer Alkoxyamines. Before performing the C−ON bond dissociation kinetic measurements, the diastereoisomeric interconversion of the dimer models was studied. As expected, in the absence of an alkyl radical scavenger the d1 and d2 isomers undergo an exchange reaction with each other upon heating with a rate coefficient k_{app}.

The kinetic scheme for the interconversion of the diastereoisomers of BSST is shown in Scheme 2. Kinetic equations describing this process have been developed by Ananchenko et al.[30] If the equilibrium experiment starts with one isomer, e.g. d1, upon heating it will experience a first-order exponential decay (eq 1) while the other isomer, d2, will grow according to a first-order exponential growth (eq 2).

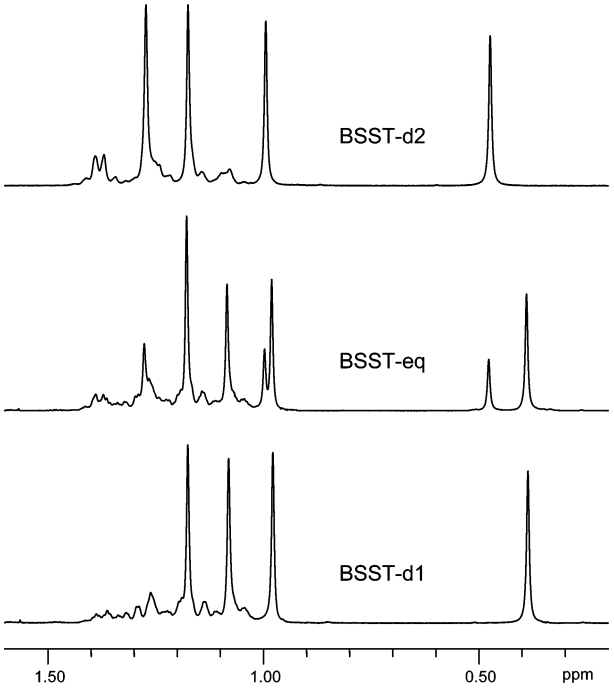

Figure 2. Partial 500 MHz ^{1}H NMR spectra from BSST diastereoisomer interconversion kinetic studies at 100 °C (top: BSST-d2 at t_0; middle: BSST-d1, BSST-d2 at equilibrium; bottom: BSST-d1 at t_0).

$$[\text{d1}] = \frac{[\text{d1}]_0 k_{c1} k_{d2}}{k_{c1} k_{d2} + k_{c2} k_{d1}} + \frac{[\text{d1}]_0 k_{c2} k_{d1} e^{-k_{app} t}}{k_{c1} k_{d2} + k_{c2} k_{d1}} \quad (1)$$

$$[\text{d2}] = \frac{[\text{d1}]_0 k_{c2} k_{d1}}{k_{c1} k_{d2} + k_{c2} k_{d1}} - \frac{[\text{d1}]_0 k_{c2} k_{d1} e^{-k_{app} t}}{k_{c1} k_{d2} + k_{c2} k_{d1}} \quad (2)$$

The dissociation rate constants are denoted as k_{d1} and k_{d2} for d1 and d2, respectively, and k_{c1} and k_{c2} are the corresponding cross-coupling rate constants. A set of equations analogous to eqs 1 and 2 can be written to describe the decay of isomer d2 and growth of d1. For both cases, the rate of isomerization is given by k_{app}, where

$$k_{app} = \frac{k_{c1} k_{d2} + k_{c2} k_{d1}}{k_{c1} + k_{c2}} \quad (3)$$

For an infinitely long time, one obtains an equilibrium between the diastereomers where the equilibrium constant, K_{eq}, is equal to

$$K_{eq} = \frac{[\text{d1}]_\infty}{[\text{d2}]_\infty} = \frac{k_{c1} k_{d2}}{k_{c2} k_{d1}} \quad (4)$$

Given K_{eq} and the individual k_d values, the k_c ratio (k_{c1}/k_{c2}) for the two isomers can be calculated.

Since the corresponding ^{1}H nuclei of the diastereoisomers have different chemical shifts, they can be readily distinguished in the NMR spectra. Experimentally, the rate of interconversion of diastereoisomers can be determined by measuring the integral ratio of any two corresponding pairs of d1 and d2 peaks. Figure 2 shows partial NMR spectra taken during the course of BSST-d1 and BSST-d2 interconversion at 100 °C. The kinetic

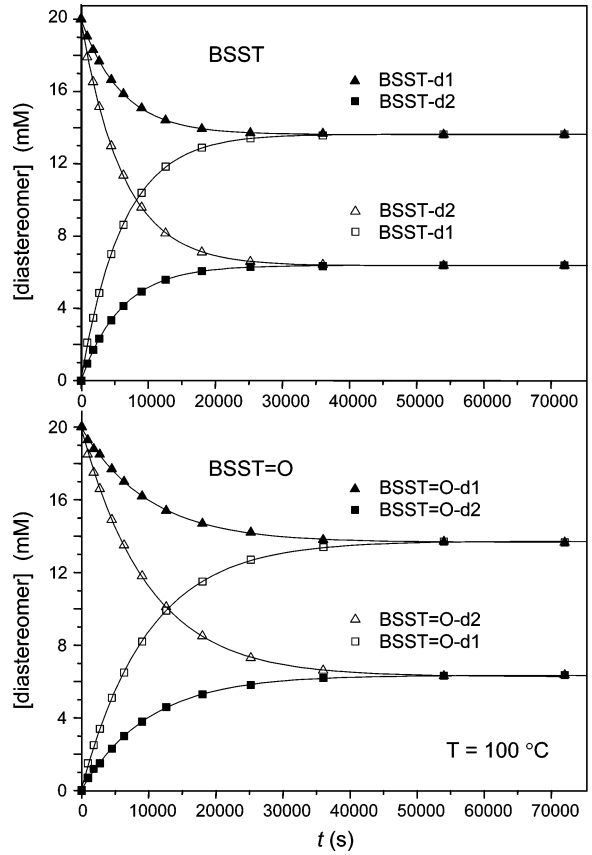

Figure 3. Diastereomer interconversion kinetic plots for BSST (top) and BSST═O (bottom) at 100 °C.

Table 1. Diastereoisomer Interconversion at 100 °C: Kinetic Data Summary

dimer	$K_{eq} = [d1]_\infty/[d2]_\infty$	k_{d2}/k_{d1}	k_{c1}/k_{c2}	k_{app} (s^{-1})	R^2
BSST-d1 decay BSST-d2 growth	2.13	2.51	0.85	1.65×10^{-4}	0.9999
BSST-d2 decay BSST-d1 growth	2.14	2.51	0.85	1.59×10^{-4}	0.9998
BSST═O-d1 decay BSST═O-d2 growth	2.15	2.31	0.93	1.00×10^{-4}	0.9995
BSST═O-d2 decay BSST═O-d1 growth	2.15	2.31	0.93	1.00×10^{-4}	0.9998
BSST-OH-eq	2.12	2.10	1.01		

parameters were quantified by monitoring the ratio of the peak intensities of the lowest frequency methyl peaks of the corresponding diastereoisomers, i.e., the peaks at 0.387 ppm for BSST-d1 and 0.474 ppm for BSST-d2 in this particular case. Figure 3 shows kinetic plots of the BSST and BSST═O diastereoisomer interconversions in the absence of an alkyl radical scavenger. The high value of the corresponding exponential line-fitting parameters R^2 (summarized in Table 1) indicates the reliability of the calculated k_{app} values. As implied by eq 3, k_{app} and k_d of a single diastereoisomer are of the same order of magnitude, provided that the values of k_c of the diastereoisomers are not significantly different due to the radical nature of the nitroxide trapping. The k_c ratios for each pair of diastereoisomers are shown in Table 1 and are seen to be similar. Therefore, the precise measurement of the k_{app} values provides valuable information on the ease of isomer exchange and good preassessment of k_d values with efficient irreversible alkyl radical trapping.

C−ON Bond Dissociation Rate Constant k_d Measurements. The dependence of the C−ON bond dissociation rate constant, k_d, on temperature was measured for three pairs of dimeric alkoxyamine diastereoisomers. From the Arrhenius plot, ln k_d vs $1/T$, the energy of activation E_a and the preexponential factor A were obtained from the slope and the intercept of the line, respectively. The results are summarized in Table 2.

Heating Time Correction for the Heat−Quench−Measure Cycle. All kinetic experiments were performed using a heat−quench−measure cycle; i.e., samples were heated in an oil bath for the prescribed time and quenched to 0 °C before measurement at 20 °C. The heating time equilibration delay (t_{corr}) was considered at the highest temperature (120 °C) at which the half-lives of the dimer models are in the range of 6−18 min. To evaluate the value of t_{corr}, eight identical 10 mM samples were prepared, heated for equally spaced prescribed times at 120 °C, and quenched; sample number one was heated for 75 s, sample number two for 150 s, and so on. The least-squares linear regression line, $\ln(I_0/I)$ vs time, was plotted. The eight-point regression line is displayed in Figure 4 with the linear fit equation $\ln(I_0/I) = -0.0173 + 9.83 \times 10^{-4} \times t$. As expected, this line does not pass through the origin. The heating delay time (t_{corr}) was calculated from the x-axis intercept, which is equal to 17.6 s.

Heating times for the BSS alkoxyamines at 120 °C were adjusted by $n \times 17.6$ s, where n denotes the number of heat−quench cycles. Correcting heating times at 110 °C or lower was deemed unnecessary since the difference in the k_d values for BSST-d1 at 110 °C, with and without time correction, was less than 1.7%.

A very important aspect of the heat−quench−measure procedure is that after quenching the ^{1}H NMR spectra are recorded at a probe temperature of 20 °C, a temperature at which the conformation of the alkoxyamine is essentially locked due to restricted C−ON bond rotation.[31] Hence, the low-frequency methyl peaks of the nitroxide moiety are well resolved due to slow exchange, enabling quantitation of the peak intensities with a high level of precision.

Pure Oxygen Trapping Efficiency and Sufficiency. To determine the true k_d values of the unimolecular C−ON bond dissociation, a trapping agent is required to capture the liberated alkyl radical efficiently and irreversibly. In this work pure oxygen was used as the trapping reagent for the alkyl radicals because trapping of a carbon-centered radical by oxygen is efficient and competes effectively with the trapping reaction with TEMPO.[32] Considering that the alkoxyamine concentration in these studies is low (0.01 mol L^{-1}), efficient oxygen trapping, at least in the initial stages of the C−ON bond dissociation reaction, could be assumed on the basis of the published solubility of oxygen in the structurally similar solvent toluene (ca. 8.64×10^{-3} mol L^{-1}, 1 atm at ambient temperature).[33] Since our kinetic experiments were carried out at elevated temperatures (80−120 °C) in *p*-xylene-d_{10}, we believed that the oxygen quenching efficiency needed to be demonstrated.[34]

One of the unique features of the ^{1}H NMR method (in contrast to ESR) is that the equilibrium between alkoxyamine diastereoisomers can be employed as a probe to test the oxygen trapping efficiency of the transient alkyl radical. The effectiveness of oxygen trapping of an alkoxyamine for up to two half-lives at 120 °C, a typical SFRP operating temperature, was experimentally proven in a unique fashion by taking advantage of the equilibrium that exists between the dimer diastereomers. The dimer interconversion experiments reported above provide a theoretical foundation for testing the trapping efficiency. Heating a pure diastereomer in the absence of a radical trap will result in the formation of an equilibrium concentration of the two diastereoisomers, readily detected by ^{1}H NMR. However, in a

Table 2. Dimer Model Arrhenius Parameters with k_d Values (Experimental and Calculated) at 120 °C

dimer	E_a (kJ/mol)[a]	A (s^{-1})[b]	R^2	k_d (s^{-1}) at 120 °C[a]	k_d(calc) (s^{-1}) at 120 °C[c]	$t_{1/2}$ (s) at 120 °C[d]
BSST-d1	139.2 ± 3.1	3.1×10^{15}	0.9985	$(9.70 \pm 0.50) \times 10^{-4}$	9.76×10^{-4}	710
BSST-d2	131.2 ± 2.4	5.5×10^{14}	0.9990	$(1.96 \pm 0.06) \times 10^{-3}$	2.00×10^{-3}	347
BSST═O-d1	143.4 ± 1.5	7.4×10^{15}	0.9998	$(6.44 \pm 0.11) \times 10^{-4}$	6.44×10^{-4}	1076
BSST═O-d2	133.7 ± 3.0	7.4×10^{14}	0.9996	$(1.27 \pm 0.05) \times 10^{-3}$	1.25×10^{-3}	555
BSST-OH-d1	138.9 ± 1.6	2.1×10^{15}	0.9990	$(7.33 \pm 0.36) \times 10^{-4}$	7.24×10^{-4}	957
BSST-OH-d2	135.7 ± 2.0	1.5×10^{15}	0.9990	$(1.37 \pm 0.07) \times 10^{-3}$	1.38×10^{-3}	502

[a] The error limits shown are standard errors of estimate for E_a and k_d from the linear least-squares fits for each parameter. [b] The standard error for ln A ranges from 0.5 for BSST═O-d1 to 1.0 for BSST-d1. [c] Calculated from the Arrhenius equation: $k_d = A \exp(-E_a/RT)$. [d] Calculated from k_d(calc) at 120 °C.

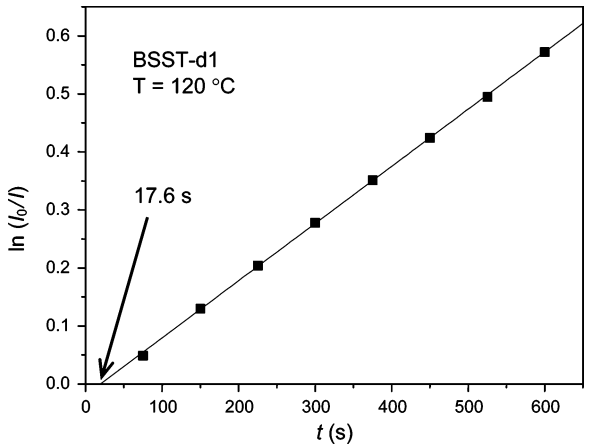

Figure 4. Heating time delay (t_{corr}) determination based on equal-time interval BSST-d1 dissociation kinetics at 120 °C.

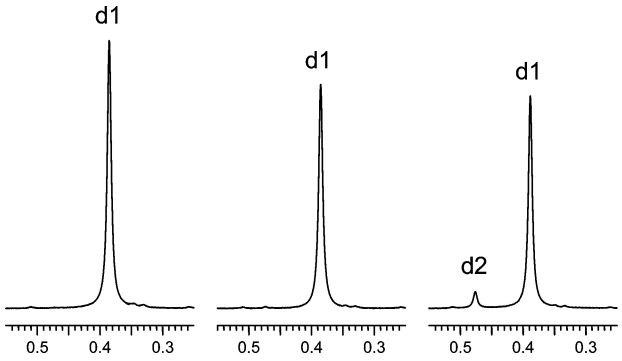

Figure 5. Partial 500 MHz ^{1}H NMR spectra demonstrating the insufficiency of oxygen in air for benzyl radical trapping in the C−ON bond homolysis of BSST-d1 (10 mM, *p*-xylene-d_{10}, 120 °C). Left: t_0 sample; middle: pure oxygen trapping after 282 s; right: air trapping after 282 s.

saturated oxygen environment no equilibration should occur since as soon as the alkyl radical is released by the homolysis of the C−ON bond, it should be immediately trapped quantitatively and irreversibly by oxygen. If this is not the case, then the diastereomeric isomer should appear. If no diastereomeric isomer is detected, then the rate of disappearance of the starting diastereoisomer will give a true value for k_d.

Figure 5 compares two ^{1}H NMR spectra taken at 282 s, less than half of one half-life of the C−ON bond dissociation reaction of BSST-d1 at 120 °C in the presence of air or pure oxygen. The inefficiency of air trapping is readily detected by the appearance of the characteristic low-frequency methyl peak for BSST-d2 at 0.474 ppm (right spectrum). With pure oxygen (middle spectrum), the peak due to BSST-d2 is greatly attenuated (<5% of the peak area with air). That the d2 peak is observed at all can be attributed to the low solubility of oxygen in *p*-xylene at elevated temperatures and a lack of mixing during the heating cycle. These effects can be minimized by reducing the concentration of alkoxyamine (2−5 mM is feasible) and

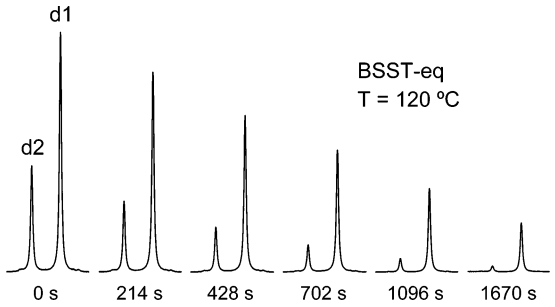

Figure 6. Sequence of partial 500 MHz ^{1}H NMR spectra taken for an equilibrated BSST sample for simultaneous measurement of BSST-d1 and BSST-d2 k_d values at 120 °C. The experimental 120 °C half-life of BSST-d1 is 715 s, and that of BSST-d2 is 354 s.

ensuring adequate mixing (gas/liquid equilibration) before each heating period. Figure 5 also demonstrates that any line-broadening effects caused by low concentrations of the two paramagnetic species in solution, oxygen and nitroxide, are not an issue as far as peak resolution is concerned, and thus high-quality peak area quantitation is achievable. Generally, by comparing a degassed sample with an O_2-charged sample, the line-broadening effect of O_2 is ca. 0.3 Hz. At 100% conversion, the concentration of released nitroxide is ca. 10 mM; the line broadening caused by this concentration of nitroxide is only 0.5 Hz.

C−ON Bond Dissociation Rate Constant k_d Measurements for Two Diastereoisomers Monitored Simultaneously. As illustrated in Figure 6, a set of methyl peaks for an equilibrium mixture of a pair of diastereoisomers are sufficiently separated that their decay over time can be used to determine k_d values simultaneously in one experiment. To determine the validity of this approach, BSST-eq was first studied. The k_d values obtained from the equilibrium mixture of diastereoisomers were compared with the individual k_d values obtained from the experiments for each separated isomer at the same temperature. The differences in k_d values for these experiments were less than 1.2% and 2.8% for BSST-d1 and BSST-d2, respectively. The ability to extract k_d values from a solution of isomeric diastereoisomers is important when the two diastereoisomers cannot be separated, as is the case for BSST-OH-eq. Applying this procedure to BSST-OH-eq gave the Arrhenius parameters and k_d values at 120 °C for BSST-OH-d1 and BSST-OH-d2 summarized in Table 2.

Kinetic Data Analysis and Reproducibility. Given that the C−ON bond dissociation reaction follows first-order kinetics, the rate constant k_d can be abstracted from the slope of the least-squares linear-regression line according to the equation $\ln I = \ln I_0 - k_d t$. To check the necessity of adding weights to every log-transformed line, we randomly selected one dimer model, BSST═O-d2 dissociation at 80 °C and obtained two k_d values: (1) $k_d = 1.18 \times 10^{-5}$ s^{-1} from weighted least-squares line fitting; (2) $k_d = 1.17 \times 10^{-5}$ s^{-1} from normal least-squares linear fitting. On the basis of the fact that the difference between the two k_d

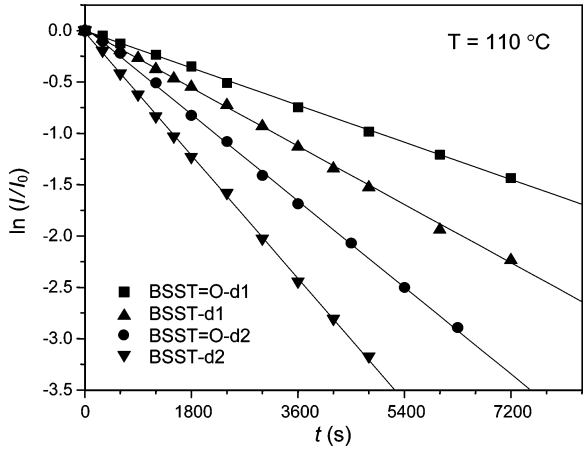

Figure 7. C−ON bond homolysis kinetic plots for BSST-d1, BSST-d2, BSST═O−d1, and BSST═O-d2 at 110 °C.

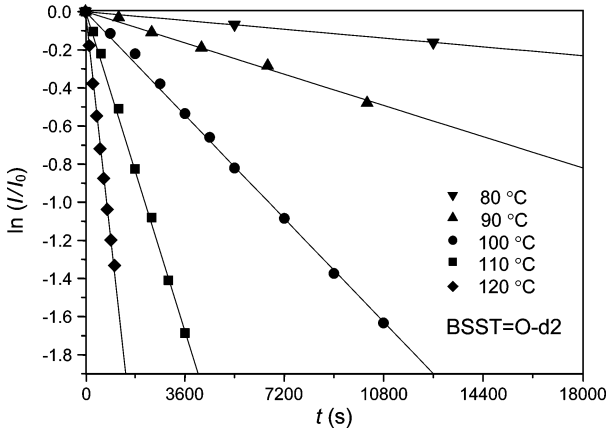

Figure 8. C−ON bond homolysis kinetic plots for BSST═O-d2 at 80, 90, 100, 110, and 120 °C. Data sets shown for 80 and 90 °C are truncated at 18 000 s for clarity.

values is 0.8%, it was concluded that the unweighted least-squares linear regression is adequate to provide reliable k_d values.

To test the reproducibility and robustness of the ^{1}H NMR method, we selected one BSS alkoxyamine, BSST-d1, and repeated the k_d measurements seven times at 120 °C under a variety of conditions (i.e., sample source, solution concentration, heating-interval spacing). For this set of samples the average k_d value was 9.70×10^{-4} s^{-1} with a standard deviation of 0.19×10^{-4} s^{-1} (relative standard deviation, 2.0%).

Comments on the Kinetic Data: k_d, E_a and A. Figure 7 demonstrates that the two isomers of each alkoxyamine dimer have different C−ON dissociation rate constants and that the k_d value of the d2 isomer is larger than that of the d1 isomer. In the temperature range 80−120 °C, for the three pairs of dimer models, k_d of d2 is approximately twice that of d1. In addition, as shown in Figure 7, the k_d value of BSST-d1 is larger than k_d for BSST═O-d1. A similar result is observed when comparing BSST-d2 with BSST═O-d2. When the results for BSST-OH are included, the following trend is observed: k_d(BSST-d1) > k_d(BSST-OH-d1) > k_d(BSST═O−d1) and k_d(BSST-d2) > k_d-(BSST-OH-d2) > k_d(BSST═O-d2). The observation that the homolysis of the 4-substituted hydroxy-alkoxyamine occurs faster than that of the corresponding ketones (referred to as the "keto effect") has previously been noted by Schulte et al.[35]

Kinetic plots, ln(I/I_0) vs t, for BSST═O-d2 at five temperatures are plotted in Figure 8.

As shown in Table 2, the frequency factors (A) of all the dimer models fall in a rather narrow range, from 7.4×10^{14} to 7.4×10^{15} s^{-1}. These values agree well with results reported by Marque et al.[16] for a large series of model compounds, wherein the preexponential factors cluster around 2.4×10^{14}. The difference in A (related to the entropy of activation) between isomers d1 and d2 is clearly shown in Figure 9. For the two diastereoisomers of BSST and BSST═O, the A values of the d1 isomers are 10 times those of the d2 isomers, whereas the activation energies of the d1 isomers are larger than those of the d2 isomers by 10 kJ/mol. This reveals that the stereochemistry of the alkoxyamine has an effect on the rate of C−ON bond dissociation. On the basis of the single-crystal structure of the two d1 isomers, in which the phenyl groups are on opposite sides of the main chain, it can be assumed that in the d2 isomers the two phenyl rings are positioned on the same side of the chain. This results in increased steric strain and contributes to the differences in the observed kinetic data. For the two diastereoisomers of BSST-OH the differences in the activation energy, the preexponential factor, and k_d values follow the same trends as those observed for BSST and BSST═O; however, the differences are much smaller.

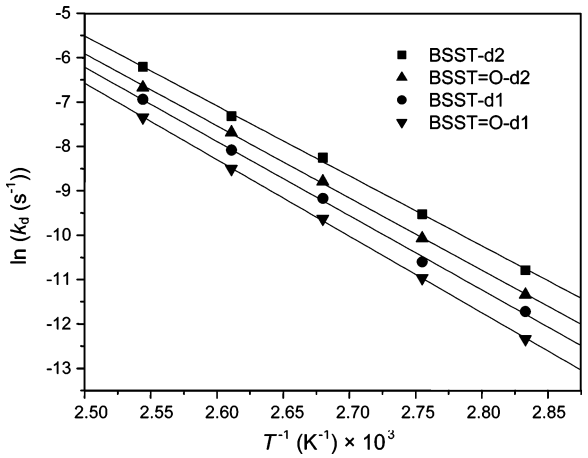

Figure 9. Arrhenius plots for the C−ON bond dissociation of BSST-d1, BSST-d2, BSST═O−d1, and BSST═O−d2 (temperatures: 80, 90, 100, 110, and 120 °C).

To validate our ^{1}H NMR method for determining k_d, we measured k_d for ST, an alkoxyamine studied previously by other methods.[14,16] Marque et al.[16] reported the following kinetic data for ST using ESR spectroscopy. Within the temperature range 90−150 °C E_a = 133.0 kJ mol^{-1}, $A = 2.5 \times 10^{14}$ s^{-1}, and $k_{d(393\ K)} = 5.2 \times 10^{-4}$ s^{-1}, whereas within the temperature range 75−120 °C E_a = 128.3 kJ mol^{-1}, $A = 0.5 \times 10^{14}$ s^{-1}, and $k_{d(393\ K)} = 4.5 \times 10^{-4}$ s^{-1}. Scaiano et al. reported kinetic values for ST obtained by HPLC methods:[14] E_a = 136.9 kJ mol^{-1}, $A = 0.4 \times 10^{14}$ s^{-1}, and $k_{d(393\ K)} = 2.5 \times 10^{-5}$ s^{-1} within the temperature range 93−154 °C. Kinetic data from our ^{1}H NMR method in the temperature range 90−130 °C are E_a = 132.3 kJ mol^{-1}, $A = 2.1 \times 10^{14}$ s^{-1}, and $k_{d(393\ K)} = 5.5 \times 10^{-4}$ s^{-1}. These values are in good agreement with the above ESR results. In addition, the reliability of the ^{1}H NMR method is demonstrated by the high consistency of the experimentally determined k_d values with the calculated ones, as shown in Table 2.

Summary

In summary, a quantitative ^{1}H NMR method has been developed to examine the k_d values of seven SFRP model compounds, including three pairs of styrene dimer alkoxyamines. The efficiency and completeness of irreversible oxygen trapping of transient alkyl radicals was first tested by taking advantage

of the existing equilibrium between the disastereoisomers of the model BSS alkoxyamines used for this study. In addition, the successful separation of pairs of diastereoisomers enabled the examination of the effect of alkoxyamine stereochemistry on the C−ON bond homolysis kinetics. The precision of the NMR method is high. Systematic errors were considered and corrected with the experimentally determined heating time correction (t_{corr}) of the heat−quench−measure cycle. The ^{1}H NMR method was validated by comparison with the ESR methods using data for a commonly examined alkoxyamine, ST. Our ^{1}H NMR method provides a general and reliable way to determine k_d values of alkoxyamines and nitroxide-terminated oligomers. It can be expanded to acrylate- and methacrylate-based alkoxyamines capped with TEMPO and its derivatives or other types of nitroxides. It has the added advantage that multiple k_d values can be determined simultaneously in a single experiment.

Acknowledgment. We gratefully acknowledge the support of NSERC Canada for a Strategic Grant and the Canada Foundation for Innovation (CFI) and Ontario Innovation Trust (OIT) for a major equipment grant. We thank Dr. Alan Lough for the X-ray crystallographic structure determinations. A preliminary account of this work was first presented at the Pacific Polymer Conference IX, Maui, Hawaii, Dec 12, 2005.

Supporting Information Available: 500 MHz ^{1}H NMR spectra of BSST-d1, BSST-d2, BSST═O-d1, BSST═O-d2, and BSST-OH. This material is available free of charge via the Internet at http://pubs.acs.org.

References and Notes

(1) (a) *Advances in Controlled/Living Radical Polymerization*; Matyjaszewski, K., Ed.; ACS Symposium Series 854; American Chemical Society: Washington, DC, 2003. (b) *Handbook of Radical Polymerization*; Matyjaszewski, K., Davis, T. P., Eds.; John Wiley and Sons: Hoboken, NJ, 2002.
(2) Solomon, D. H.; Rizzardo, E.; Cacioli, P. U.S. Patent 4,581,429, 1986.
(3) (a) Georges, M. K.; Veregin, R. P. N.; Kazmaier, P. M.; Hamer, G. K. *Macromolecules* **1993**, *26*, 2987−2988. (b) Georges, M. K.; Veregin, R. P. N.; Kazmaier, P. M.; Hamer, G. K. U.S. Patent 5,322,912, 1994.
(4) Solomon, D. H. *J. Polym. Sci., Part A: Polym. Chem.* **2005**, *43*, 5748−5764.
(5) Hawker, C. J.; Bosman, A. W.; Harth, E. *Chem. Rev.* **2001**, *101*, 3661−3688.
(6) Wang, J.-S.; Matyjaszewski, K. *J. Am. Chem. Soc.* **1995**, *117*, 5614−5615.
(7) Matyjaszewski, K.; Xia, J. *Chem. Rev.* **2001**, *101*, 2921−2990.
(8) Chiefari, J.; Chong, Y. K. B.; Ercole, F.; Krstina, J.; Jeffery, J.; Le, T. P. T.; Mayadunne, R. T. A.; Meijs, G. F.; Moad, C. L.; Moad, G.; Rizzardo, E.; Thang, S. H. *Macromolecules* **1998**, *31*, 5559−5562.
(9) Barner-Kowollik, C.; Davis, T. P.; Heuts, J. P. A.; Stenzel, M. H. V. P.; Whittaker, M. *J. Polym. Sci., Part A: Polym. Chem.* **2003**, *41*, 365−375.
(10) Moad, G.; Mayadunne, R. T. A.; Rizzardo, E.; Skidmore, M.; Thang, S. H. *Kinetics and Mechanism of RAFT Polymerization*; Matyjaszewski, K., Ed.; *ACS Symp. Ser.* **2003**, *854*, 520−535.
(11) (a) Fischer, H. *Macromolecules* **1997**, *30*, 5666−5672. (b) Fischer, H. *J. Polym. Sci., Part A: Polym. Chem.* **1999**, *37*, 1885−1901. (c) Fischer, H. *Criteria for Livingness and Control in Nitroxide-Mediated and Related Radical Polymerizations*; Matyjaszewski, K., Ed.; *ACS Symp. Ser.* **2003**, *854*, 10−23.
(12) (a) Souaille, M.; Fischer, H. *Macromolecules* **2000**, *33*, 7378−7394. (b) Souaille, M.; Fischer, H. *Macromolecules* **2001**, *34*, 2830−2838. (c) Souaille, M.; Fischer, H. *Macromolecules* **2002**, *35*, 248−261.
(13) (a) Goto, A.; Fukuda, T. *Prog. Polym. Sci.* **2004**, *29*, 329−385. (b) Fukuda, T.; Yoshikawa, C.; Kwak, Y.; Goto, A.; Tsujii, Y. *Mechanisms and Kinetics of Living Radical Polymerization: Absolute Comparison of Theory and Experiment;* Matyjaszewski, K., Ed.; *ACS Symp. Ser.* **2003**, *854*, 24−39. (c) Fukuda, T. *J. Polym. Sci., Part A: Polym. Chem.* **2004**, *42*, 4743−4755.
(14) Skene, W. G.; Belt, S. T.; Connolly, T. J.; Hahn, P.; Scaiano, J. C. *Macromolecules* **1998**, *31*, 9103−9105.
(15) Moad, G.; Rizzardo, E. *Macromolecules* **1995**, *28*, 8722−8728.
(16) Marque, S.; Le Mercier, C.; Tordo, P.; Fischer, H. *Macromolecules* **2000**, *33*, 4403−4410.
(17) Bon, S. A. F.; Chambard, G.; German, A. L. *Macromolecules* **1999**, *32*, 8269−8276.
(18) Veregin, R. P. N.; Georges, M. K.; Hamer, G. K.; Kazmaier, P. M. *Macromolecules* **1995**, *28*, 4391−4398.
(19) Goto, A.; Terauchi, T.; Fukuda, T.; Miyamoto, T. *Macromol. Rapid Commun.* **1997**, *18*, 673−681.
(20) Goto, A.; Fukuda, T. *Macromolecules* **1997**, *30*, 5183−5186.
(21) Fukuda, T.; Goto, A. *Macromol. Rapid Commun.* **1997**, *18*, 683−688.
(22) Ballesteros, O. G.; Maretti, L.; Sastre, R.; Scaiano, J. C. *Macromolecules* **2001**, *34*, 6184−6187.
(23) Bertin, D.; Gigmes, D.; Marque, S.; Tordo, P. *e-Polym.* **2003**, *002*, 1−9.
(24) Fischer, H. *Chem. Rev.* **2001**, *101*, 3581−3610 and references therein.
(25) Moffat, K. A.; Hamer, G. K.; Georges, M. K. *Macromolecules* **1999**, *32*, 1004−1012.
(26) Skene, W. G.; Scaiano, J. C.; Yap, G. P. A. *Macromolecules* **2000**, *33*, 3536−3542.
(27) Berger, S.; Braun, S. *200 and More NMR Experiments*; Wiley-VCH Verlag GmbH & Co. KGaA: Weinheim, Germany, 2004.
(28) (a) *MestReC*, Mestrelab Research S.L.; Santiago de Compostela, A Coruna, Spain. (b) Cobas, J. C.; Sardina, F. J. *Concepts Magn. Reson., Part A* **2003**, *19A*, 80−96.
(29) Georges, M. K.; Hamer, G. K.; Listigovers, N. A. *Macromolecules* **1998**, *31*, 9087−9089.
(30) Ananchenko, G. S.; Souaille, M.; Fischer, H.; Mercier, C. L.; Tordo, P. *J. Polym. Sci., Part A: Polym. Chem.* **2002**, *40*, 3264−3283.
(31) Anderson, J. E.; Corrie, E. T. *J. Chem. Soc., Perkin Trans. 2* **1992** 1027−1031.
(32) Moad, G.; Solomon, D. H. *The Chemistry of Free Radical Polymerization*, 1st ed.; Elsevier Science Ltd.: Amsterdam, 1995.
(33) *IUPAC Solubility Data Series*; Battino, R., Ed.; Pergamon Press: New York, 1981; Vol. 7.
(34) In previous ESR studies of k_d, Marque et al.[16] and Bon et al.[17] demonstrated the efficiency of oxygen for trapping alkyl radicals derived from alkoxyamines using air instead of pure O_2.
(35) Schulte, T.; Studer, A. *Macromolecules* **2003**, *36*, 3078−3084.

MA061700C